

Overlapping binary and multiple open cluster candidates in the Galaxy

G. Javakhishvili and M. Todua

Georgian National Astrophysical Observatory, Ilia State University, Kazbegi ave. 2a, 0160 Tbilisi, Georgia

A few binary open clusters with visually separable components are known in the Galaxy. However there can be dual systems that overlap in the line of sight and are seen as a single cluster. On the basis of the WEBDA database we studied the V-band magnitude distributions of stars of the open clusters in the Galaxy. Most of these distributions showed Gaussian-like shape with a single peak, but some of them demonstrated two and more peaks which we considered as a manifestation of duality or multiplicity of the object. We examined the magnitude distributions of 563 rich open clusters from the WEBDA database with more than 100 stars and revealed 70 of them with two and more statistically significant peaks which we considered as binary and multiple cluster candidates. On the basis of these clusters we comprised a catalogue of possible binary and multiple clusters in the Galaxy overlapping in the line of sight. Geometric centres of cluster components and corresponding numbers of cluster members were estimated.

I. INTRODUCTION

Studies of binary and multiple clusters are interesting from the point of view of star formation and evolution in galaxies. A possible mechanism of formation of double stellar systems had been suggested by Fujimoto & Kumai [1997], and further developed by Bekki et al. [2004], where cloud-cloud collisions were considered as the most feasible way to produce two or more clusters. A different scenario was proposed by Leon et al. [1999] considering a tidal capture.

These theories were introduced after the detection of binary clusters in the Large and Small Magellanic Clouds (LMC and SMC) in Bhatia & Hatzidimitriou [1988], Hatzidimitriou & Bhatia [1990], and references therein. A significant fraction, of open clusters in the Magellanic Clouds (MCs) were found in pairs, with the maximum projected separation between the centers of the components 18.7 pc. The number of found pairs was greater than expected from projection effects. It was also suggested that some of the binary cluster candidates were physical pairs. A catalogue with a photographic atlas of the binary system candidates in the LMC was compiled by Bhatia et al. [1991]. Some of these objects possibly were triple systems and some of the binary cluster candidates were imbedded in molecular clouds. Hatzidimitriou & Bhatia [1990] catalogued the cluster pairs in the SMC. Dieball et al. [2002] further developed this research and presented a new catalogue of binary and multiple cluster candidates in the LMC.

In our Galaxy χ and h Persei (NGC 869 and NGC 884) had been for a long time the only distinguishable binary open cluster, until Subramanyam et al. (1995) detected 18 probable binary systems with spatial separations between the components of up to 20 pc. Out of these, 16 pairs had members that seemed to have similar ages, which might suggest that they were physical pairs. This suggestion was based on the ages and radial velocities of the member clusters. These studies revealed that the fraction of clusters in pairs in the Galaxy was significantly smaller than that in the MC: 9% from the 400 clusters investigated by Subramaniam et al. (1995), 27% of the 4089 clusters investigated by Dieball et al. (2002).

All pairs in the above studies were visually separable. However, it is possible that some cluster pairs overlap in the line of sight and it is difficult or impossible to resolve them. Thus they are seen as single clusters. Some of them might be physical pairs, some not. Galadi-Enriquez et al. [1998] considered NGC 1750 and 1758 as overlapping open clusters, although they suggested that this pair did not make up a gravitationally bound system.

Studying open clusters from the WEBDA database for membership determination using the accumulation method, described in Javakhishvili et al. [2006], we examined the distributions of V-band magnitudes of cluster members. Most of these distributions displayed Gaussian-like asymmetric shape with a single peak. However some of them revealed two and more distinct peaks, at which we decided to take a closer look. We propose that this feature of magnitude distributions could indicate duality or multiplicity of the open cluster systems overlapping in the line of sight.

II. THE METHOD

There are 938 open clusters in the WEBDA database with available rectangular positions (hpd type) of the member stars. Among them we choose 563 rich clusters with more than 100 members to examine the distributions of V-magnitude of stars in each cluster. Limiting magnitudes of stars varied for different clusters from $m_V = 13$ to 25. Most of the V-magnitude distributions showed a typical Gaussian-like form with a single peak. However the

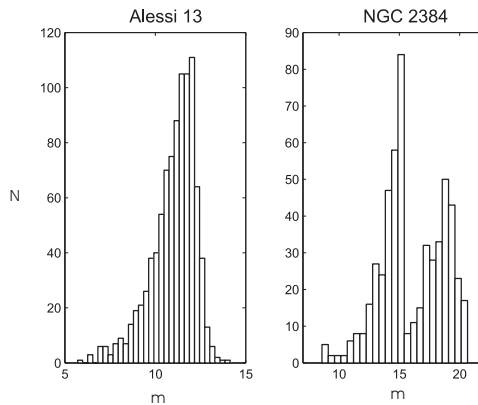


FIG. 1: V-magnitude distributions of clusters Alessi 13 and NGC 2384.

V-magnitude distributions of about 70 clusters displayed two and more "humps". Fig. 1 illustrates two examples of these distributions. The first one - Alessi 13 - has a single magnitude peak, which is typical for 88% of the chosen rich clusters. The second one - NGC 2384 - exhibits two distinct peaks. We propose that one of the explanations for this kind of profile can be two clusters overlapping due to projection effect. If this is the case, then they might be either close physical systems or separate clusters projected along the same line of sight. Since the probability of the latter is less than 1 (Subramanyam et al. % [1995]), it is likely that most of them are physically associated.

Binary open clusters projected on the sky can be seen with separated members like η and χ Persei, but some of them should overlap, one being behind another, so that the components cannot be resolved (Fig. 2 within the volume ABCD). Assuming the maximum distance between the centres of the two clusters to be 20 pc and equal sizes of the constituents, we estimated the probability that an arbitrary pair is seen as an overlapping cluster:

$$p = \frac{V_{ABCD}}{V_{sphere}} 100\% \quad (1)$$

This probability depends on the sizes of the components and is plotted in Fig. 3. According to this plot, for example, about 70% of the binary clusters, each of the members of which have diameters about 3 pc should be seen to an observer as overlapped and thus as a single cluster, and all the clusters with diameters > 10 pc should overlap.

The characteristic asymmetric profile of the V-magnitude distribution of an open cluster, like Alessi 13, can be well fitted by the extreme value distribution (EVD) function. The profile similar to that of NGC 2384 with two (or more) peaks can be best adjusted by the combination of two (or more) EVD functions:

$$f(m) = \sum \frac{A_i}{\sigma_i} e^{\frac{m-\mu_i}{\sigma_i}} e^{-e^{\frac{m-\mu_i}{\sigma_i}}} \quad (2)$$

$i = 1, 2, \dots, n$, where n is the number of components, μ_i is a centre of EVD for i -th component, A_i is the fitted coefficient, and σ_i the standard deviation. Two EVD functions with different centres and their superposition are shown in Fig. 4.

III. DISCUSSION

A. General discussion

All 70 clusters with two and more "humps" in their V-magnitude distributions were processed and fitted by the combination of EVD functions (eq. 2). The goodness of fits were in the range of 0.8 to 0.98. These clusters were compiled into a catalogue presented in Tables 1 and 2. With our criteria, we found 56 binary, 12 triple and 2 quadruple overlapping cluster candidates.

The number of stars in the i -th cluster member was determined as

$$N_i = \sum f_i(m_j) \quad (3)$$

where f_i is the EVD function for the i -th cluster, j runs the bin numbers of the i -th cluster.

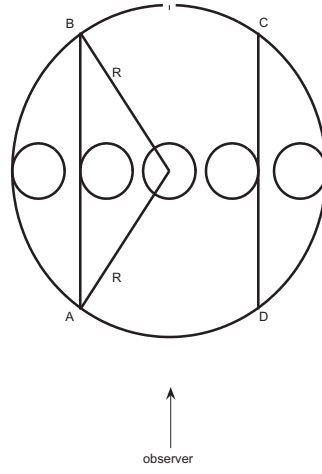


FIG. 2: For estimation of the probability to see an overlapping binary cluster. The radius of the big circle $R=20\text{pc}$, the diameters of small circles are 3pc .

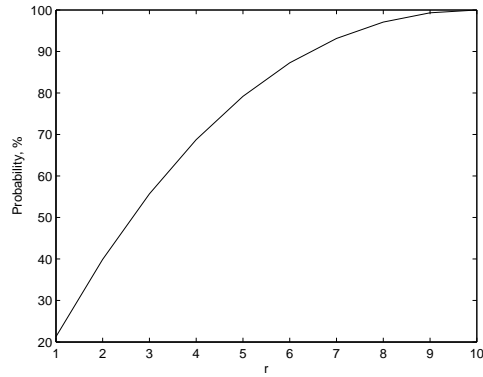


FIG. 3: Fraction of the overlapping binary clusters among all binary cluster candidates depending on the radii (r) of the components.

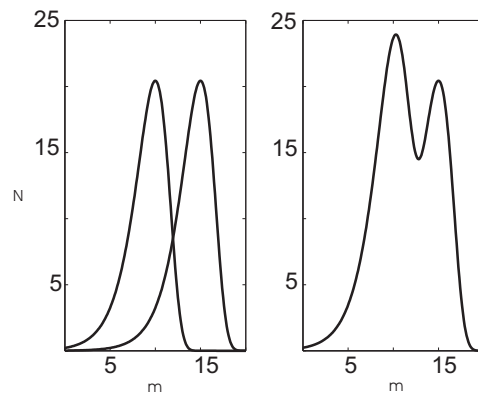


FIG. 4: Extreme value distribution functions: two single distributions (left) and their superposition (right).

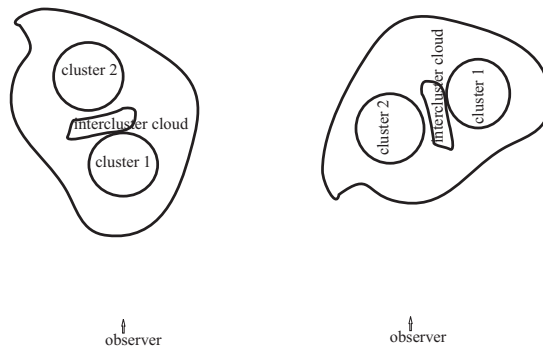


FIG. 5: Two possible orientations of a binary open cluster imbedded in a molecular cloud (outer curve). The binary cluster members are represented by circles, separated by an intercluster cloud. These configurations produce different magnitude distributions.

Discrepancies between the total number of stars N and the sum of the calculated numbers of stars in the members were

$$\Delta N\% = \left| \frac{N - \sum N_i}{N} * 100 \right| \quad (4)$$

which characterize the uncertainty of belonging of some stars to either components.

Geometrical centres of the clusters and those of the i -th companion were determined as

$$X_0 = \frac{\sum x_j}{N}, \quad Y_0 = \frac{\sum y_j}{N}, \quad j = 1, \dots, N \quad (5)$$

$$X_i = \frac{\sum x_j p_i(m)}{N_i}, \quad Y_i = \frac{\sum y_j p_i(m)}{N_i} \quad (6)$$

where p_i is the probability for a star with magnitude m to belong to the i -th component:

$$p_i(m) = \frac{f_i(m)}{\sum f_k(m)}, \quad i, k = 1, \dots, n \quad (7)$$

The differences in magnitude peaks $\Delta\mu$ range from 1.5 to 8, the majority of them falling between 1.5 and 3 (see Fig. 10). Differences in intensities between the two structures are

$$\Delta I = 2.512^{\Delta\mu} \quad (8)$$

For $\Delta\mu = 4$, as in the case of NGC 2384 in Fig. 1 (which is a young cluster at a distance of about 2 kpc) $\Delta I \approx 40$ which means that the distance modulus of the components differ by about 6 times. If we assume that there is an absorption cloud between the two structures, then their separation will be considerably smaller. Young clusters are located in large molecular clouds (Efremov [1986]). Some binary cluster candidates in the catalogue of Bhatia et al. [1991] were imbedded in clouds. In this case $\Delta\mu$ could be due to the inter-cluster cloud absorption. When a cluster formation starts in two parts of a giant molecular cloud, a light pressure from young stars drives out the rest of the cloud. These fragments could be kept by the gravity of the clusters and concentrate in the libration zones, thus forming the dense absorptive clouds, which could be responsible for $\Delta\mu$. Though in some cases, if there is another cluster nearby, the second peak can appear due to stars of this cluster. This might be true for the magnitude distribution of NGC 2384, shown on the Fig. 1, which has a nearby cluster NGC 2383. As was stated in Piskunov et al. [2004], the central part of NGC 2384 might be relatively free from contamination from NGC 2383, it is possible that the farer parts of it might not.

Various configurations of projections of clusters and inter-cluster clouds (Fig. 5) result in different magnitude profiles. In the case of the configuration when one companion is behind another separated by a molecular cloud (on the left diagram in Fig. 5), an observer sees a single cluster instead of two, but the magnitude distribution shows two peaks. In the case of the configuration on the right in Fig. 5 one sees a visually separable double cluster.

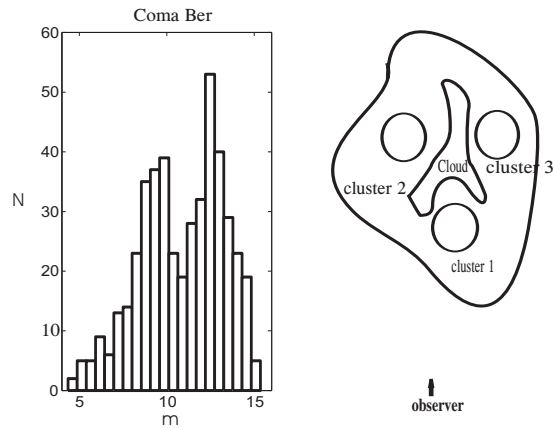


FIG. 6: V-magnitude distribution of stars in Coma Ber open cluster (left) and one of the possible configurations accounting for this histogram (right).

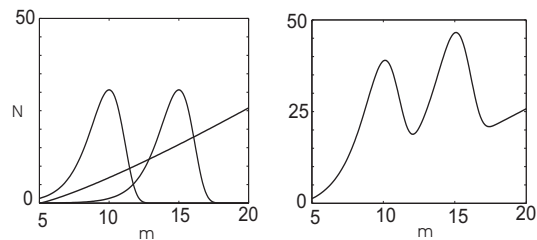


FIG. 7: Two components of a binary cluster plus background stars (left) and their combination (right).

We encountered two cases of the double-peak magnitude distributions: when the first peak is higher than the second, and vice versa. If the second peak is higher than the first (the case of Coma Berenices cluster, Fig. 6), it can indicate that either (a) the rare cluster is more populous than the front one, or (b) there are two or more clusters in the rare (right picture on Fig. 6), or (c) the tail of the rare cluster is "contaminated" by a large number of background stars, and therefore it looks richer (Fig. 7).

We would like to point out the case of NGC 6633. Fig. 8 shows how the combination of "cluster + background stars" can result in the magnitude distribution like that of NGC 6633 (Fig. 9). For the real distribution we used two different fittings shown in Fig. 9: one with the "cluster + background stars" combination (left diagram), and the usual combination of two EVDs (right diagram). In both cases the goodness of fits were high, though it seems that the second peak is due to the background stars.

Selection effects and incompleteness of data also can affect magnitude distributions. To determine the probable cause of the double peak in a magnitude histogram - either duality, or neighbouring cluster, or background/foreground stars, each case must be studied individually.

The differences of magnitude centres of the clusters from our list vary from $\Delta\mu = 1$ to 8. Fig. 10 demonstrates the

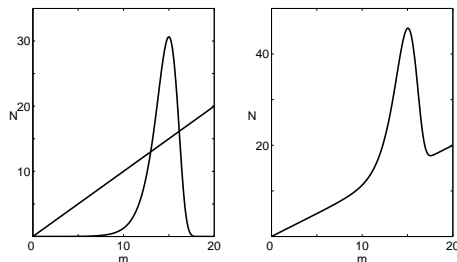


FIG. 8: A possible configuration for the magnitude distribution of NGC 6633: the second peak is due to "contamination" by background stars.

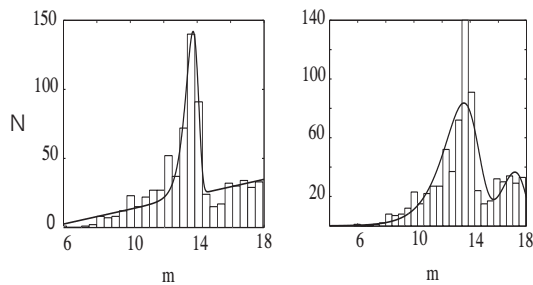


FIG. 9: The magnitude distribution of stars in NGC 6633 with two different fittings: "cluster + background stars" (left) and "cluster + cluster" (right).

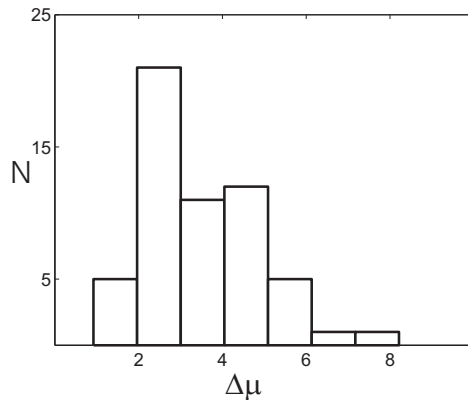


FIG. 10: Distribution of differences of the magnitude centres $\Delta\mu$ in overlapping binary open cluster candidates.

distribution of this value, where $\Delta\mu \approx 3$ is dominant.

In Fig. 11 the distribution of ages of overlapping double and multiple open clusters in our list are presented, demonstrating that clusters of all ages are presented almost evenly, about 50% being young objects.

B. The case of Coma Berenices cluster

Studying probable duality or multiplicity of open clusters we considered only V-magnitude distributions for consistency and the maximum data completeness, since the V-band data were available for all objects. However many

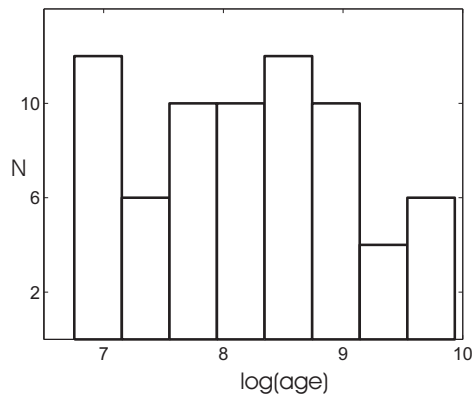


FIG. 11: Age distribution of overlapping double and multiple open cluster candidates.

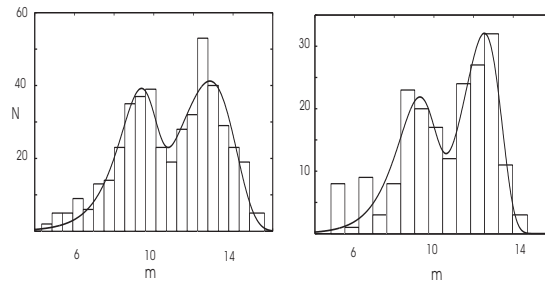


FIG. 12: V-magnitude distributions of stars in Coma Ber open cluster and its EVD fits: for all stars listed in WEBDA (left) and for the stars after membership determination (right).

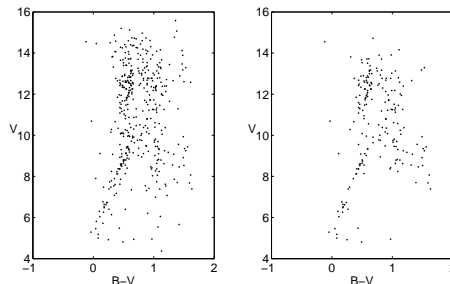


FIG. 13: Color-magnitude diagrams of Coma Ber open cluster: for all stars listed in WEBDA (left) and for the stars after membership determination (right).

clusters in our list have measurements in other filters too. We consider here one particular case with measurements in B-band, usually available for brighter stars. We present an example of Coma Berenices (or Melotte 111) cluster as a typical case of an overlapping double open cluster candidate in more detail. The distance to the object is 96 pc - this is the second closest cluster in our list. It is a young cluster ($\log(\text{age}) = 8.7$) and 459 stars are listed in the WEBDA database.

The V-magnitude distribution of Coma Berenices cluster with its EVD fit is demonstrated in Fig. 12 (left diagram). The peaks appear at $\mu = 9.2$ and 12.5 . The difference between the magnitudes $\Delta\mu = 3.3$ is typical for most of the members of our list. The goodness of fit is 0.87. To exclude background stars we used the accumulation method for determination of cluster membership by Javakhishvili et al. [2006], selecting the stars with close proper motions. Thus the number of cluster members (having both proper motions and $B - V$), with probability more than 90%, were 198. The corresponding V-magnitude distribution (Fig. 12, right diagram) also reveals dual feature of the cluster around almost the same magnitude peaks $\mu = 9.3$ and 12.7 . This indicates that stars around these peaks have similar proper motions, thus they possibly are physically associated.

In Fig 13 the color-magnitude diagrams (CMD) of the cluster are presented, for all stars (right diagram) and cluster members after membership determination (left diagram). Double feature also can be seen in these CMDs and around the same V-magnitudes $\mu = 9$ and 13 , which can be one more argument in favour of duality of Coma Ber open cluster, the components of which are visually overlapped.

IV. SUMMARY

In addition to the visually separable binary open cluster candidates in the Galaxy found by Subramaniam et al. (1995), there might be pairs that overlap in the line of sight and are seen as single clusters. On the basis of the WEBDA database we investigated open clusters in the Galaxy considering the distributions of the V-magnitudes of cluster members. Those clusters that demonstrated two or more magnitude peaks were regarded as candidates for overlapping binary and multiple systems. We found that these distributions can be well fitted by combinations of two or more extreme value distribution functions. We examined the V-magnitude distributions of 563 clusters from the

WEBDA for which more than 100 members are listed and revealed that 70 of them have more than one peaks and considered them as binary and multiple cluster candidates. On the basis of these assumptions we compiled a catalogue of the overlapping binary and multiple cluster candidates of the Galaxy. Geometric centres of the component clusters and corresponding numbers of stars were estimated.

Acknowledgement. In this paper we made use of the WEBDA database. We would like also to thank Dr. G. Didebulidze for useful comments and suggestions.

-
- [2004] Bekki, K., Beasley, M. A., Forbes, D. A., Couch, W. J. 2004, ApJ, 602, 730
[1988] Bhatia, R. K., Hatzidimitriou, D. 1988, MNRAS, 230, 215
[1991] Bhatia, R. K., Read, M. A., Tritton, S., Hatzidimitriou, D. 1991, A&AS, 87, 335
[2002] Dieball, A., Muller, H., Grebel, E. K. 2002, A&A, 391, 547
[1986] Efremov, Y. N. 1986, Astronomicheskij tsirkulyar, 1447
[1997] Fujimoto, M., Kumai, Y. 1997, AJ, 113, 249
[1998] Galadi-Enriquez, D., Jordi, C., Trullols, E., and Ribas, I. 1998, A&A, 333, 471
[2006] Javakhishvili, G., Kukhianidze, V., Todua, M., Inasaridze, R. 2006, A&A, 447, 3, 915
[1990] Hatzidimitriou, D., Bhatia, R. K. 1990, A&A, 230, 11
[1999] Leon, S., Bergond, G., Vallenari, A. 1999, A&A, 344, 450
[2004] Piskunov, A. E.; Belikov, A. N.; Kharchenko, N. V.; Sagar, R.; Subramaniam, A. 2004, MNRAS, 349, 1449
[1995] Subramaniam, A., Gorti, U., Sagar, R., Bhatt, H.C. 1995 A&A, 302, 86
[2007] WEBDA catalogues <http://www.univie.ac.at/webda>

TABLE I: List of the overlapping binary and multiple cluster candidates in the Galaxy. General information: cluster identifier, right ascension, declination, Galactic latitude and longitude, angular diameter, distance and logarithm of age.

cluster identifier	$\alpha(2000)$ h m s	$\delta(2000)$ o / ' / "	l o	b o	diameter /	distance pc	log(age)
Binary clusters							
NGC 129	00 30 00	+60 13 06	120.270	-2.543	19.0	1625	7.9
NGC 188	00 47 28	+85 15 18	122.843	22.384	17.0	2047	9.6
King 2	00 51 00	+58 11 00	122.874	-4.688	5.0	5750	9.8
NGC 381	01 08 19	+61 35 00	124.939	-1.223	6.0	1148	8.5
NGC 659	01 44 24	+60 40 24	129.375	-1.534	5.0	1938	7.5
NGC 869	02 19 00	+57 07 42	134.632	-3.741	18.0	2079	7.1
NGC 884	02 22 18	+57 08 12	135.052	-3.582	18.0	2345	7.0
NGC 1039	02 42 05	+42 45 42	143.658	-15.613	35.0	499	8.2
NGC 1245	03 14 42	+47 14 12	146.647	-8.931	9.0	2876	8.7
IC 348	03 44 30	+32 17 00	160.490	-17.802	7.0	385	7.6
NGC 1750	05 03 55	+23 39 30	179.178	-10.695	20.0	630	8.3
NGC 1817	05 12 15	+16 41 24	186.156	-13.096	16.0	1972	8.6
Berkeley 17	05 20 36	+30 36 00	175.646	-3.648	7.0	2700	10.1
NGC 1912	05 28 40	+35 50 54	172.250	0.695	20.0	1066	8.5
NGC 1960	05 36 18	+34 08 24	174.535	1.072	10.0	1318	7.5
NGC 2099	05 52 18	+32 33 12	177.635	3.091	14.0	1383	8.5
NGC 2129	06 00 41	+23 19 06	186.555	0.056	5.0	1515	7.3
NGC 2158	06 07 25	+24 05 48	186.634	1.781	5.0	5071	9.0
Berkeley 73	06 22 00	-06 21 00	215.278	-9.424	2.0	15	9.4
Collinder 110	06 38 24	+02 01 00	209.649	-1.978	18.0	1950	9.2
Dolidze 25	06 45 06	+00 18 00	211.942	-1.273	20.0	6304	6.8
NGC 2301	06 51 45	+00 27 36	212.558	0.279	14.0	872	8.2
Tombaugh 1	07 00 29	-20 34 00	232.334	-7.314	5.0	3000	9.0
NGC 2384	07 25 10	-21 01 18	235.390	-2.393	5.0	2116	6.9
Berkeley 39	07 46 42	-04 36 00	223.462	10.095	7.0	4780	9.9
NGC 2506	08 00 01	-10 46 12	230.564	9.935	12.0	3460	9.0
NGC 2539	08 10 37	-12 49 06	233.705	11.112	9.0	1363	8.6
NGC 2682	08 51 18	+11 48 00	215.696	31.896	25.0	908	9.4
NGC 2818	09 16 01	-36 37 30	261.980	8.584	9.0	1855	8.6
NGC 3114	10 02 36	-60 07 12	283.332	-3.840	35.0	911	8.1
NGC 3324	10 37 20	-58 38 30	286.228	-0.188	12.0	2317	6.8
Collinder 228	10 42 04	-59 55 00	287.668	-1.047	14.0	2201	6.8
NGC 3680	11 25 38	-43 14 36	286.764	16.919	5.0	938	9.1
Coma Ber	12 25 06	+26 06 00	221.353	84.025	120.0	96	8.7
Collinder 272	13 30 26	-61 19 00	307.595	1.202	10.0	2045	7.2
NGC 5606	14 27 47	-59 37 54	314.841	0.994	3.0	1805	7.1
NGC 6025	16 03 17	-60 25 54	324.551	-5.884	14.0	756	7.9
NGC 6087	16 18 50	-57 56 06	327.726	-5.426	14.0	891	8.0
NGC 6204	16 46 09	-47 01 00	338.560	-1.040	5.0	1085	7.6
NGC 6253	16 59 05	-52 42 30	335.460	-6.251	4.0	1510	9.7
Ruprecht 130	17 47 32	-30 06 00	359.221	-0.960	3.0	2100	7.7
NGC 6451	17 50 41	-30 12 36	359.478	-1.601	7.0	2080	8.1
NGC 6494	17 57 04	-18 59 06	9.894	2.834	29.0	628	8.5
NGC 6633	18 27 15	+06 30 30	36.011	8.328	20.0	376	8.6
NGC 6649	18 33 27	-10 24 12	21.635	-0.785	5.0	1369	7.6
Basel 1	18 48 12	-05 51 00	27.355	-1.947	5.0	2178	7.9
NGC 6811	19 37 17	+46 23 18	79.210	12.015	14.0	1215	8.8
IC 4996	20 16 30	+37 38 00	75.353	1.306	6.0	1732	6.9
Berkeley 86	20 20 24	+38 42 00	76.667	1.272	6.0	1112	7.1
NGC 6910	20 23 12	+40 46 42	78.683	2.013	10.0	1139	7.1
NGC 6939	20 31 30	+60 39 42	95.903	12.304	10.0	1185	9.3
NGC 6940	20 34 26	+28 17 00	69.860	-7.147	25.0	770	8.9
IC 5146	21 53 24	+47 16 00	94.383	-5.495	20.0	852	8.0
NGC 7243	22 15 08	+49 53 54	98.857	-5.524	29.0	808	8.1
NGC 7510	23 11 03	+60 34 12	110.903	0.064	6.0	2075	7.6
Markarian 50	23 15 18	+60 28 00	111.350	-0.225	2.0	2114	7.1
Triple clusters							
NGC 663	01 46 09	+61 14 06	129.467	-0.941	14.0	1952	7.2
Berkeley 66	03 04 18	+58 46 00	139.434	0.218	4.0	5200	9.7
NGC 1976	05 35 16	-05 23 24	209.010	-19.386	47.0	399	7.1
NGC 2204	06 15 33	-18 39 54	226.014	-16.107	10.0	2629	8.9
Haffner 6	07 20 06	-13 08 00	227.861	0.258	6.0	3054	8.8
NGC 2420	07 38 23	+21 34 24	198.107	19.634	5.0	3085	9.0
NGC 2437	07 41 46	-14 48 36	231.858	4.064	20.0	1375	8.4
NGC 2571	08 18 56	-29 45 00	249.106	3.532	8.0	1342	7.5
Praesepe	08 40 24	+19 40 00	205.920	32.484	70.0	187	8.9
NGC 5617	14 29 44	-60 42 42	314.670	-0.100	10.0	1533	7.9
NGC 5662	14 35 37	-56 37 06	316.937	3.394	29.0	666	8.0
NGC 7788	23 56 45	+61 23 54	116.434	-0.782	4.0	2374	7.6
Quadruple clusters							
NGC 2548	08 13 43	-05 45 00	227.873	15.393	30.0	769	8.6
NGC 6709	18 51 18	+10 19 06	42.120	4.715	14.0	1075	8.2

TABLE II: List of the overlapping binary cluster candidates in the Galaxy. Characteristics: total number of stars (N), number of stars in the components (N_i), discrepancy between the total number of stars and the sum of numbers of stars in the components ($\Delta N\%$), geometrical centres of the system (X_0, Y_0) and its components (X_i, Y_i), difference of the magnitude centres ($\Delta\mu$). For triple and quadruple clusters $N_{3,4}$, $X_{3,4}$, $Y_{3,4}$ and $\Delta\mu$ between 2nd and 3rd and 3rd and 4th components are given in the second row of the appropriate cluster.

cluster identifier	N	N_1	N_2	$\Delta N\%$	X_0	Y_0	X_1	Y_1	X_2	Y_2	$\Delta\mu$
Double clusters											
NGC 129	2272	1227	1044	0.1	48.85	20.75	6.12	60.85	42.73	-40.10	4.8
NGC 188	10584	1767	8674	1.4	-88.38	180.61	-14.52	46.40	-73.86	134.21	4.7
King 2	1037	644	393	0.0	-23.65	-3.78	-19.75	-1.63	-3.90	-2.15	2.2
NGC 381	2897	1283	1553	2.1	-40.56	43.25	-10.98	27.93	-29.58	15.32	2.2
NGC 659	764	209	556	0.1	-18.11	7.89	-4.69	4.56	-13.42	3.33	4.8
NGC 869	3754	3029	549	4.7	-9.99	-2.62	-8.49	-2.19	-1.49	-0.43	0.9
NGC 884	3293	2617	521	4.7	10.93	-2.12	8.68	-1.32	2.25	-0.81	1.0
NGC 1039	993	667	319	0.7	0.17	-88.56	-20.87	-67.97	21.04	-20.60	2.1
NGC 1245	1016	614	353	4.8	13.11	8.92	9.58	4.40	3.53	4.52	2.5
IC 348	1929	430	1506	0.5	4.05	20.97	1.08	3.22	2.97	17.75	4.5
NGC 1750	7416	4392	2592	5.8	-0.37	0.51	1.90	0.66	-2.27	-0.15	3.0
NGC 1817	1891	1428	474	0.6	20.19	-75.36	8.82	-49.52	11.37	-25.84	3.5
Berkeley 17	5393	4336	1124	1.2	-32.42	-23.22	-22.39	-25.77	-10.03	2.55	3.5
NGC 1912	1274	304	994	1.9	-3.17	-12.09	-1.18	-4.61	-1.99	-7.48	2.4
NGC 1960	1394	719	664	0.8	-0.37	1.53	2.44	-0.00	-2.80	1.53	4.3
NGC 2099	5027	1068	3891	1.4	1.43	-1.97	-0.12	0.06	1.55	-2.02	2.4
NGC 2129	863	259	584	2.3	-25.67	5.22	-9.75	3.12	-15.92	2.10	5.9
NGC 2158	5359	1498	3897	0.7	-0.84	12.14	5.92	5.12	-6.76	7.02	1.2
Berkeley 73	367	73	292	0.5	-146.22	92.88	-15.52	23.29	-130.70	69.59	2.2
Collinder 110	2006	616	1430	2.0	-60.18	-173.05	-18.32	-29.13	-41.86	-143.92	3.5
Dolidze 25	136	29	106	0.7	79.32	33.77	-7.71	60.85	87.03	-27.08	5.8
NGC 2301	1611	1002	568	2.6	33.47	-1.60	17.64	-7.53	15.83	5.94	2.7
Tombaugh 1	1970	1193	740	1.9	294.07	239.12	232.01	188.79	62.06	50.33	3.0
NGC 2384	549	235	268	8.4	-6.49	5.47	19.87	0.97	-26.36	4.50	4.1
Berkeley 39	4408	1642	2794	0.6	-45.72	15.86	-21.24	15.83	-24.48	0.02	3.0
NGC 2506	1232	217	1021	0.5	2.13	-7.26	1.31	-0.79	0.82	-6.48	2.1
NGC 2539	821	356	473	1.0	0.50	-34.47	-1.94	-21.17	2.44	-13.31	4.3
NGC 2682	3284	2255	1025	0.1	-0.09	-2.49	-0.01	-2.13	-0.08	-0.36	4.4
NGC 2818	1168	188	976	0.3	-11.25	-8.19	-0.93	-2.37	-10.32	-5.83	3.6
NGC 3114	2119	230	1847	2.0	-18.41	55.30	-1.04	4.98	-17.37	50.33	8.7
NGC 3324	988	626	376	1.4	-24.02	138.98	-5.99	70.31	-18.03	68.67	4.3
Collinder 228	1471	328	1087	3.8	-67.11	15.21	4.77	11.51	-71.88	3.70	6.0
NGC 3680	888	733	70	9.6	-1.41	-2.93	-2.02	-2.78	0.61	-0.14	1.3
Coma Ber	459	142	305	2.6	159.96	-18.32	23.07	4.06	136.89	-22.38	3.6
Collinder 272	1826	786	990	2.7	129.61	-12.88	89.05	-34.81	40.56	21.93	2.9
NGC 5606	202	69	130	1.5	-3.23	-8.36	-0.14	-7.14	-3.09	-1.22	3.9
NGC 6025	182	153	29	0.0	0.25	-13.13	-2.11	-9.69	2.35	-3.44	3.0
NGC 6087	1393	662	686	3.2	2.37	-4.88	1.49	-4.32	0.88	-0.55	4.0
NGC 6204	523	141	369	2.5	83.31	9.39	39.96	11.65	43.35	-2.26	3.6
NGC 6253	8194	3207	4742	3.0	68.86	43.48	73.60	31.36	-4.74	12.12	3.5
Ruprecht 130	523	310	211	0.4	106.95	-70.14	86.08	-82.54	20.86	12.40	2.5
NGC 6451	1491	1128	322	2.8	-15.84	-82.21	-19.00	-78.95	3.16	-3.26	2.1
NGC 6494	332	256	82	1.8	-3.27	-3.90	-0.52	-1.76	-2.75	-2.15	2.4
NGC 6633	759	259	513	1.7	5.90	5.13	0.21	-0.79	5.69	5.92	2.6
NGC 6649	517	125	396	0.8	2.39	7.71	1.24	4.18	1.16	3.53	3.9
Basel 1	1297	732	550	1.2	0.14	79.64	26.99	65.48	-26.85	14.16	2.1
NGC 6811	430	367	52	2.6	26.35	17.61	26.62	16.08	-0.27	1.53	1.3
IC 4996	775	175	600	0.0	43.49	51.38	9.49	-2.29	34.00	53.67	4.7
Berkeley 86	736	204	518	1.9	-7.64	2.10	-8.54	2.64	0.90	-0.54	5.9
NGC 6910	401	147	250	1.0	3.41	2.81	0.14	0.21	3.27	2.60	3.4
NGC 6939	2870	424	2495	1.7	-33.32	22.21	7.33	0.27	-40.66	21.93	6.8
NGC 6940	1054	710	349	0.5	0.70	0.76	0.29	0.85	0.41	-0.09	5.1
IC 5146	856	659	174	2.7	0.72	-12.21	4.49	-8.76	-3.77	-3.45	3.0
NGC 7243	3194	882	2329	0.5	-2.89	6.71	-0.56	0.23	-2.33	6.48	2.0
NGC 7510	839	152	705	2.2	-2.25	6.01	-0.60	1.65	-1.65	4.36	2.9
Markarian 50	1262	375	886	0.1	18.20	9.09	6.13	0.47	12.06	8.62	4.7

TABLE III: List of the overlapping triple and quadruple cluster candidates in the Galaxy. Characteristics: total number of stars (N), number of stars in the components (N_i), discrepancy between the total number of stars and the sum of numbers of stars in the components ($\Delta N\%$), geometrical centres of the system (X_0, Y_0) and its components (X_i, Y_i), difference of the magnitude centres ($\Delta\mu$). For triple and quadruple clusters $N_{3,4}$, $X_{3,4}$, $Y_{3,4}$ and $\Delta\mu$ between 2nd and 3rd and 3rd and 4th components are given in the second row of the appropriate cluster.

cluster identifier	N	N_1	N_2	$\Delta N\%$	X_0	Y_0	X_1	Y_1	X_2	Y_2	$\Delta\mu$
Triple clusters											
NGC 663	4560	345 1874	2282	1.3	-21.74	1.74	-1.82 -11.00	-1.55 6.06	-8.93	-2.77	3.6 2.8
Berkeley 66	1677	329 813	521	0.8	-67.44	-91.00	-76.44 10.68	28.73 -79.17	-1.69	-40.56	3.0 2.0
NGC 1976	6034	1387 296	4357	0.1	-567.48	-97.37	-266.45 0.18	-72.67 0.84	-301.21	-25.53	3.5 6.7
NGC 2204	2468	649 1305	503	0.5	5.99	15.30	-1.15 7.15	2.68 8.05	-0.02	4.57	2.3 1.9
Haffner 6	711	77 535	92	1.0	-9.57	21.01	0.56 -8.96	2.29 15.43	-1.18	3.29	2.3 2.0
NGC 2420	942	204 360	357	2.2	8.95	1.18	1.86 -0.30	-1.41 -2.44	7.40	5.03	2.0 1.9
NGC 2437	1687	459 817	409	0.1	70.18	55.90	5.98 48.27	4.54 38.43	15.93	12.93	2.9 2.2
NGC 2571	1710	127 145	1416	1.3	-128.80	2.53	-2.97 -12.14	1.49 0.31	-113.70	0.74	5.4 1.7
Praesepe	1689	816 323	513	2.2	-21.30	-115.95	-2.75 0.00	-60.44 -0.00	-18.56	-55.51	4.3 2.5
NGC 5617	1447	381 742	317	0.5	-9.36	-5.81	-7.04 -2.40	-1.55 -0.62	0.08	-3.64	2.9 2.1
NGC 5662	978	190 436	334	1.8	0.29	-0.54	-0.23 0.07	-0.54 -0.03	0.45	0.03	2.3 4.8
NGC 7788	424	120 211	88	1.2	-44.80	-63.55	20.09 -46.33	-28.62 -26.23	-18.56	-8.70	1.8 1.3
Quadruple clusters											
NGC 2548	2247	112 516	445 1200	1.2	-9.52	-9.48	-0.22 -3.96	1.32 -4.02	-3.86 -1.48	-1.39 -5.38	2.0 1.8 3.3
NGC 6709	1921	196 216	223 1276	0.5	1.38	-1.60	-0.22 0.31	0.43 0.12	1.01 0.27	-0.92 -1.23	1.6 0.8 2.9